

Anti-apoptosis Proteins Mcl-1 and Bcl-xL Have Different p53-Binding Profiles

Hongwei Yao,^{†,‡,¶} Shuofu Mi,^{‡,¶} Weibin Gong,[†] Jian Lin,[‡] Nuo Xu,[‡] Sarah Perrett,[†] Bin Xia,[‡] Jinfeng Wang,^{*,†} and Yingang Feng^{*,†,§}

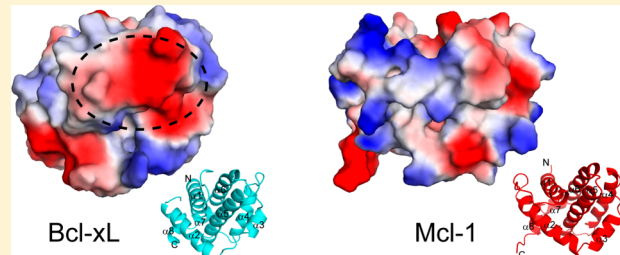
[†]National Laboratory of Biomacromolecules, Institute of Biophysics, Chinese Academy of Sciences, 15 Datun Road, Beijing 100101, China

[‡]Beijing Nuclear Magnetic Resonance Center, College of Chemistry and Molecular Engineering, Peking University, Beijing 100871, China

[§]Shandong Provincial Key Laboratory of Energy Genetics, Qingdao Institute of Bioenergy and Bioprocess Technology, Chinese Academy of Sciences, Number 189 Songling Road, Qingdao 266101, China

^{*}MOE Key Laboratory of Bioinformatics, School of Life Sciences, Tsinghua University, Beijing 100084, China

ABSTRACT: One of the transcription-independent mechanisms of the tumor suppressor p53 discovered in recent years involves physical interaction between p53 and proteins of the Bcl-2 family. In this paper, significant differences between the interaction of p53 with Mcl-1 and Bcl-xL were demonstrated by NMR spectroscopy and isothermal titration calorimetry. Bcl-xL was found to bind strongly to the p53 DNA-binding domain (DBD) with a dissociation constant (K_d) of ~ 600 nM, whereas Mcl-1 binds to the p53 DBD weakly with a dissociation constant in the mM range. In contrast, the p53 transactivation domain (TAD) binds weakly to Bcl-xL with a $K_d \sim 300\text{--}500 \mu\text{M}$ and strongly to Mcl-1 with a $K_d \sim 10\text{--}20 \mu\text{M}$. NMR titrations indicate that although the p53 TAD binds to the BH3-binding grooves of both Bcl-xL and Mcl-1, Bcl-xL prefers to bind to the first subdomain (TAD1) in the p53 TAD, and Mcl-1 prefers to bind to the second subdomain (TAD2). Therefore, Mcl-1 and Bcl-xL have different p53-binding profiles. This indicates that the detailed interaction mechanisms are different, although both Mcl-1 and Bcl-xL can mediate transcription-independent cytosolic roles of p53. The revealed differences in binding sites and binding affinities should be considered when BH3 mimetics are used in cancer therapy development.



The tumor suppressor p53 mediates cell apoptosis by targeting the transcriptional activity of a large number of genes.^{1,2} In addition to its well-established functions as a nuclear transcription factor, transcription-independent mechanisms have been found in recent years by which p53 can promote apoptosis in the cytosol and mitochondria.^{3–6} One of these transcription-independent mechanisms involves the physical interaction between p53 and Bcl-2 family proteins.^{3,6} The Bcl-2 family contains anti-apoptotic members as well as pro-apoptotic members, which regulate apoptosis and tumorigenesis by their complex interaction network.^{7,8} The Bcl-2 protein family members share sequence homology in several conserved regions known as Bcl-2 homology (BH) domains. The anti-apoptotic members (such as Bcl-2, Bcl-xL, and Mcl-1) as well as some pro-apoptotic members (such as Bak and Bax) contain three or four BH domains and share a similar overall fold. Other pro-apoptotic members (such as Bim and Bid), termed BH3-only proteins, contain only the third BH domain, which binds to the BH3-binding groove of anti-apoptotic Bcl-2 family members. The anti-apoptotic function of Bcl-2 family members is generally achieved by complex formation with pro-apoptotic Bcl-2 family members, thus inhibiting their mitochondrial apoptosis function.⁷ Several models have been

proposed for the transcription-independent mechanisms of p53 on the basis of the interactions between p53 and different Bcl-2 family members.^{3,6} In one model, p53 directly interacts with pro-apoptotic Bak and Bax and activates them in mitochondria to induce apoptosis.^{9,10} In another model, p53 is proposed to have roles similar to BH3-only proteins, which interact with anti-apoptotic Bcl-2 proteins and liberate pro-apoptotic Bak or Bim from the complexes.¹¹ A recent study added anti-apoptotic Mcl-1 into this scheme with the discovery that direct interaction between p53 and Mcl-1 accompanies the disruption of the Mcl-1 and Bim complex.¹² In spite of the importance of the p53 and Bcl-2 interactions, the detailed interaction mode is unclear and some controversial models have been proposed.³

Mcl-1 is a distinct anti-apoptotic member of the Bcl-2 family because of its special physical and physiological characteristics, though Mcl-1 has a very similar core structure and shows many similar functions to other anti-apoptotic Bcl-2 proteins. Mcl-1 contains only three BH domains, whereas Bcl-2 and Bcl-xL

Received: November 21, 2012

Revised: August 26, 2013

Published: August 26, 2013

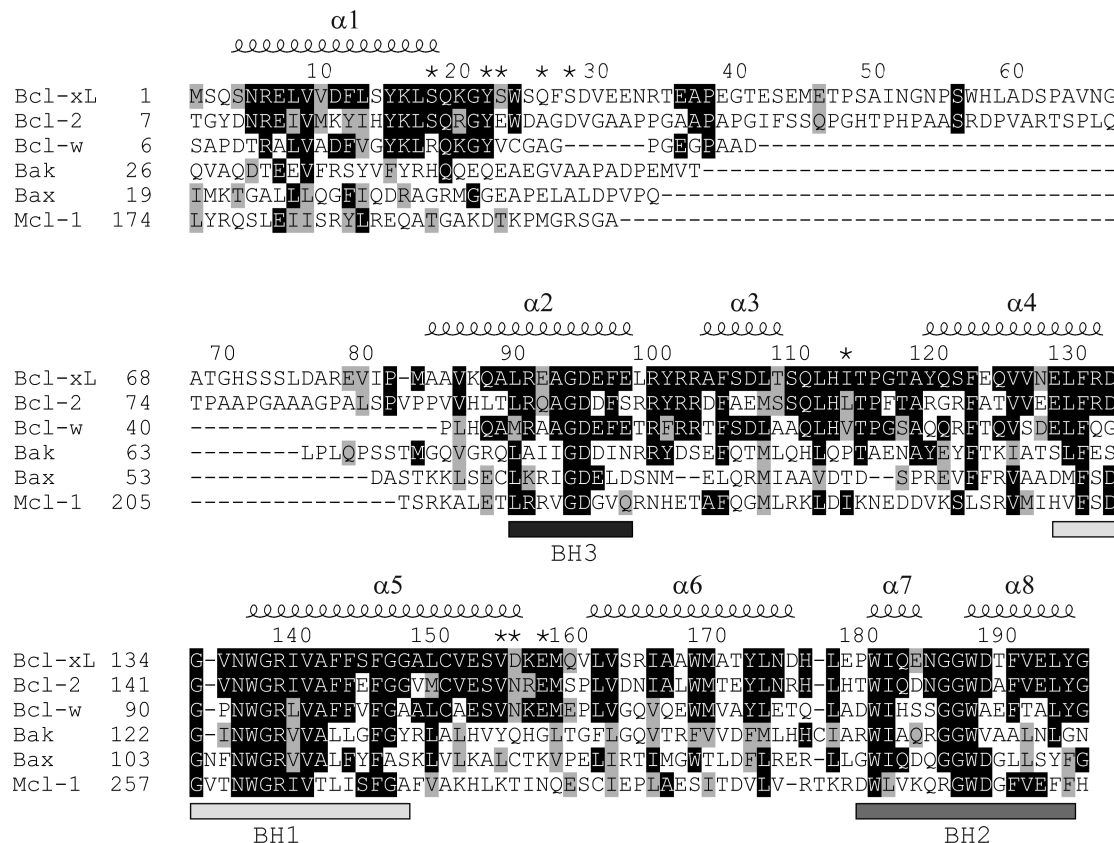


Figure 1. Sequence alignment of Bcl-2 family members including anti-apoptotic members Bcl-xL, Bcl-2, Bcl-w, and Mcl-1 as well as pro-apoptotic members Bak and Bax. The key residues of the p53 DBD-binding sites for Bcl-xL are indicated by asterisks.

each contain four BH domains, and Mcl-1 shares only about 25% sequence identity with other family members.¹³ Mcl-1 has a very short half-life, probably due to its long N-terminal flexible regulatory region (~170 amino acid residues), which is not present in other Bcl-2 members.¹⁴ Mcl-1 has a significantly different BH3 binding profile^{13,15,16} and is identified as a major source of resistance to the BH3-mimic drug-candidate compound ABT-737, which binds to Bcl-2 and Bcl-xL but not to Mcl-1.^{17–19} Recent studies have shown that Mcl-1 has distinct functions from other anti-apoptotic Bcl-2 members, such as its essential role in germinal center formation and B cell memory,²⁰ a stress sensor role in regulating autophagy,²¹ and synergism with p53 in protecting from hepatic injury, fibrosis, and cancer.²²

Previous studies have shown that both Bcl-xL and Mcl-1 can interact with p53, which emphasizes the similarity of the two interactions.¹² The interaction between p53 and Bcl-xL has been studied more extensively, but a thorough comparison of p53 binding profiles for Bcl-xL and Mcl-1 has not yet been described. Previous studies showed that two domains of p53, the DNA-binding domain (DBD, residues 94–312) and the transactivation domain (TAD, residues 1–73), are able to bind to Bcl-xL,^{11,23} but which of these domains has more physiological importance is still under debate.³ The binding site of Bcl-xL to the p53 DBD identified by NMR spectroscopy is a negatively charged region (involving the C-terminus of helix α1, the N-terminus of the loop between helices α1 and α2, the loop between helices α3 and α4, the loop between helices α5 and α6, and the N-terminus of helix α6), and the binding is mediated through electrostatic interactions.^{24,25} However, the binding surface in Bcl-xL is not conserved in

Mcl-1 (Figure 1). The TAD of p53 binds to the BH3-binding groove of Bcl-xL²⁶ and to other Bcl-2 family members including Mcl-1, Bcl-2, and Bcl-w,²⁷ but it is known that Mcl-1 and Bcl-xL have different BH3 binding profiles.^{13,15} Therefore, the p53 binding sites on Bcl-xL are not well conserved in Mcl-1. However, no experimental study reported so far has addressed whether or not Mcl-1 and Bcl-xL have the same p53-binding profiles. Careful comparison of the interaction profiles will provide further insight into the role of Bcl-2 family proteins in the transcription-independent apoptosis mechanism of p53.

In this paper, we studied the interaction profile of p53 with Mcl-1 compared to that of p53 with Bcl-xL. The p53-binding profile of Mcl-1 was found to be quite different from that of Bcl-xL, although both Mcl-1 and Bcl-xL could directly interact with p53. Unlike the strong interaction between Bcl-xL and the p53 DBD, only a very weak interaction was detected between Mcl-1 and the p53 DBD involving a different binding surface; thus, the latter may not be a physiologically relevant interaction. However, Mcl-1 can bind to the p53 TAD with a much stronger affinity than Bcl-xL, suggesting that the p53 TAD, not the DBD, is the physiological binding site for Mcl-1. Further, in the p53 TAD, Bcl-xL prefers to bind to the first subdomain (TAD1), whereas Mcl-1 prefers to bind to the second subdomain (TAD2). These different p53-binding profiles of Bcl-xL and Mcl-1 provide further insight into the transcription-independent mechanism of p53, which indicates a new aspect that should be considered in drug design.

EXPERIMENTAL PROCEDURES

Cloning, Expression, and Protein Purification. The DNA fragment encoding the core domain (residues 171–327)

of human Mcl-1 was cloned into a modified version of the pGBO vector²⁸ into which an additional PreScission protease cleavage site was introduced between the His₆-GB1 fusion partner and Mcl-1. The plasmid was transformed into *Escherichia coli* Rosetta (DE3) to produce the protein. Uniformly ¹⁵N- and ¹⁵N/¹³C-labeled Mcl-1 were expressed in M9 medium with ¹⁵N-NH₄Cl and [¹³C]-glucose as the sole nitrogen and carbon sources, respectively. After cells were grown to an *A*₆₀₀ of 0.6–0.8 at 37 °C, the protein production was induced with 1 mM isopropyl-β-D-thiogalactopyranoside, and the cells were grown for a further 3 h. Proteins were first purified by nickel-affinity chromatography and then cleaved with PreScission protease in 50 mM Tris-HCl (pH 8.0), 150 mM NaCl overnight at 4 °C. The cleavage mixture was then passed through a nickel-affinity column. The fraction containing Mcl-1 was collected and further purified using a Superdex 75 gel filtration chromatography column. The purified protein was dialyzed against 100 mM NH₄HCO₃ and then lyophilized and stored at –20 °C. The same protocol was also used to clone and purify the core domain of human Bcl-xL (a truncated construct lacking the transmembrane domain and the flexible loop between helices α1 and α2²⁴).

To express the p53 TAD (residues 1–73), TAD1 (residues 1–40), and TAD2 (residues 37–61), the corresponding DNA fragments were also cloned into the modified version of the pGBO vector.²⁹ The expression and purification procedures were the same as for Mcl-1, except that the cells were grown at 37 °C to an *A*₆₀₀ of 0.6–0.8, shifted to 16 °C before induction with 0.1 mM isopropyl-β-D-thiogalactopyranoside, and further grown for 20–24 h. The p53 DBD (residues 94–312) was produced and purified in a similar manner as described²⁴ using the vector pET1Sb containing the p53 DBD DNA fragment between the NdeI and XhoI restriction sites.

Nuclear Magnetic Resonance (NMR) Spectroscopy. All NMR spectra were recorded on a Bruker DMX600 spectrometer equipped with a *z*-gradient triple-resonance cryoprobe. Data were processed with Felix (Accelrys Inc.) and analyzed with NMRViewJ.³⁰ The chemical shifts in the spectra were referenced to internal 2,2-dimethyl-2-silapentane-5-sulfonate.

Backbone resonance assignments for Bcl-xL and Mcl-1 were derived from the two-dimensional ¹H–¹⁵N heteronuclear single quantum correlation (HSQC) experiment and the three-dimensional ¹H–¹³C–¹⁵N HNCA, HNCACB, and CBCA(CO)NH experiments (all of which were acquired at 308 K), referring to the previously reported assignments.^{31,32} Backbone resonance assignments for the p53 TAD were obtained from the two-dimensional ¹H–¹⁵N HSQC experiment and the three-dimensional ¹H–¹³C–¹⁵N HNCACB, CBCA(CO)NH, HNCO, and HNCA experiments performed at 298 K, and the resonance assignments for the p53 TAD at 308 K were obtained by observing the gradual shift in the cross peaks in the 2D ¹H–¹⁵N HSQC spectra with increase in temperature from 298 to 308 K. NMR titration of Bcl-xL and Mcl-1 with each of the p53 DBD and the p53 TAD, as well as the reverse titration of the p53 TAD with each of Mcl-1 and Bcl-xL, were performed by recording ¹H–¹⁵N HSQC spectra at 308 K. Samples for titration experiments were prepared in 95/5% (v/v) H₂O/D₂O containing 50 mM potassium phosphate (pH 6.5) and 100 mM KCl. The composite chemical shift perturbations upon ligand binding were calculated according to the equation³³ $\Delta\delta = [(\Delta\delta_H^2 + \Delta\delta_N^2/25)/2]^{1/2}$, where Δδ_H and Δδ_N are the chemical shift perturbations for ¹H and ¹⁵N resonances,

respectively. The equilibrium dissociation constants were derived by fitting the chemical shift perturbations to an equation assuming a single site binding model as described.³⁴

In addition, for analysis of the binding site of p53 on Mcl-1, a model of human Mcl-1 was built from the mouse Mcl-1 protein (PDB code 1WSX, with 89% identity)³⁵ using Modeller³⁶ because no human Mcl-1 structure in free state has so far been reported.

Isothermal Titration Calorimetry (ITC). A binary ITC experiment was used to detect the interaction of the p53 TAD and the p53 DBD with each of Mcl-1 and Bcl-xL. All ITC experiments were performed on an iTC₂₀₀ microcalorimeter (MicroCal Inc.). Titrations between Mcl-1 or Bcl-xL and the p53 TAD were performed in 50 mM potassium phosphate (pH 6.5), 100 mM KCl at 25 °C. For the Mcl-1 and p53 TAD titration, 0.14 mM Mcl-1 was placed in the sample chamber and 1.5 mM p53 TAD was added by syringe in 20 successive additions of 2 μL each (with an initial injection of 0.5 μL). For the Bcl-xL and p53 TAD titration, 0.1 mM Bcl-xL was placed in the sample chamber and 3.6 mM p53 TAD was added by syringe in 20 successive additions of 2 μL each (with an initial injection of 0.5 μL). Titrations between Mcl-1 or Bcl-xL and the p53 DBD were performed in 50 mM potassium phosphate (pH 7.2), 150 mM KCl, 5 mM β-mercaptoethanol at 20 °C. A solution of 0.03 mM p53 DBD was placed in the sample chamber and 0.3 mM Bcl-xL or Mcl-1 was added by syringe in 20 successive additions of 2 μL each (with an initial injection of 0.5 μL). All protein solutions were dialyzed against the corresponding buffer and degassed before each experiment. Protein concentrations were determined by absorbance at 280 nm. The heat of dilution was subtracted from the calorimetric data. Titration data were analyzed with the software Origin (MicroCal Inc.) using a single-site binding model.

Fluorescence Polarization. Fluorescence polarization (FP) measurements of the Bcl-xL interaction with the p53 DBD were performed according to the procedure described by Hagn et al.²⁴ The experiments were performed at 18 °C using a RF-5301 PC spectrofluorophotometer (SHIMADZU, Japan). Labeling of Bcl-xL was done according to the manufacturer's protocol using 5',6'-carboxyfluorescein succinimidyl ester (Molecular Probes, Invitrogen), and the free label was removed by passage over a PD-10 desalting column (GE Healthcare). Labeling yields were ~50%. Fluorescein-labeled Bcl-xL (400 nM) was titrated with increasing amounts (0.4–100 μM) of p53DBD proteins in 20 mM sodium phosphate, pH 7.2. FP was measured using the appropriate filter for fluorescein excitation and detection (excitation = 488 nm, emission = 523 nm). The dissociation constant was obtained by fitting the data to a single-site binding model.

RESULTS

p53 DNA-Binding Domain Has Different Binding Affinities and Sites for Mcl-1 and Bcl-xL. Interaction of the p53 DBD with Bcl-xL is well established,^{11,24} but whether the p53 DBD also interacts with Mcl-1 remains unclear. To investigate this, NMR titration experiments were performed with ¹⁵N-labeled Mcl-1 in the absence and presence of unlabeled p53 DBD. A number of peaks in the ¹H–¹⁵N HSQC spectrum of Mcl-1 were slightly perturbed in the titration with the p53 DBD (Figure 2F). The perturbed regions of Mcl-1 are mainly around the BH3-binding groove of Mcl-1 (Figure 2G,I). However, the dissociation constant could not be derived from the very small chemical shift perturbation because

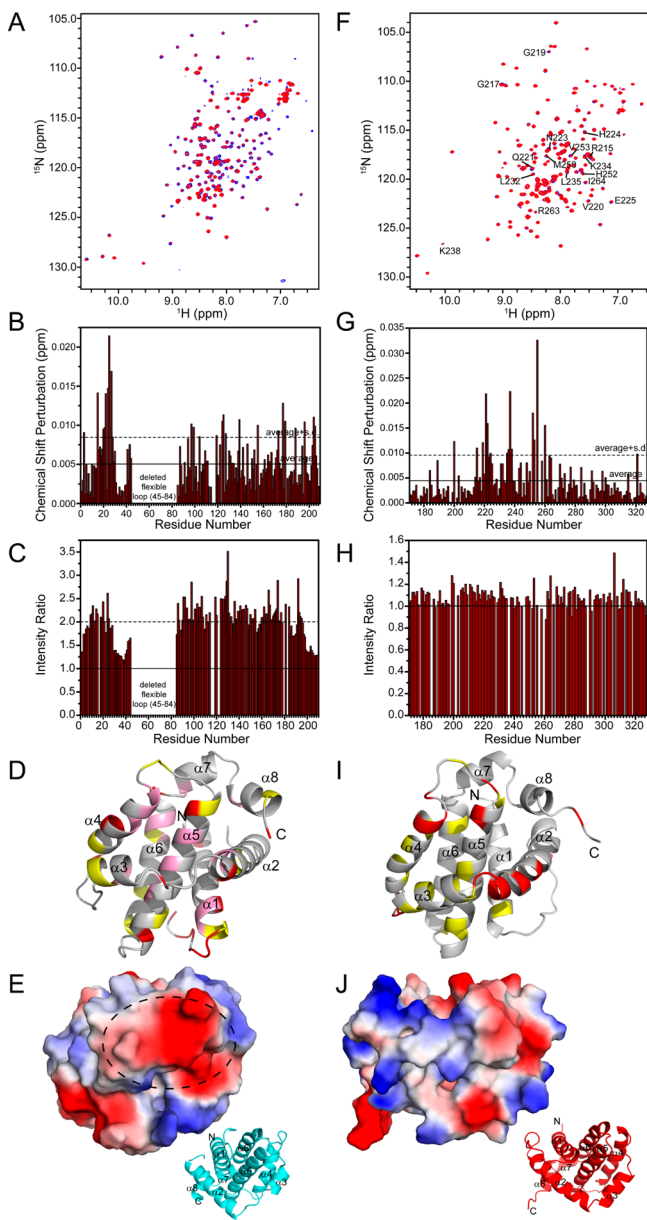


Figure 2. NMR titrations characterizing the different p53-DBD-binding modes of Bcl-xL and Mcl-1. (A–E) Bcl-xL. (F–J) Mcl-1. (A, F) ^1H - ^{15}N HSQC spectra of the titrations. (B, G) Chemical shift perturbations (CSP) versus residue number. (C, H) Peak intensities versus residue number. (D, I) Structural mappings of the chemical shift perturbations. Residues with a CSP value more than the average CSP value plus one standard deviation (average + s.d., dashed line in panels B and G) are shown in red; those with a CSP value between the average CSP value (average, solid line in panels B and G) and the average CSP value plus one standard deviation are shown in yellow. Buried perturbed residues in Bcl-xL are shown in pink. (E, J) Electrostatic potential surface of the p53 DBD-binding site on Bcl-xL (E) and the corresponding surface on Mcl-1 (J). Positive and negative charges are shown in blue and red, respectively. Ribbon representations are also shown to indicate the orientations of Bcl-xL and Mcl-1 in the surface representations.

saturating conditions could not be attained. This means that the binding affinity between Mcl-1 and the p53 DBD is extremely weak and is therefore most likely not physiologically relevant.

The weak interaction between the p53 DBD and Mcl-1 is very different from the interaction with Bcl-xL reported

previously.³⁷ To verify this difference, the interaction between Bcl-xL and the p53 DBD was also studied by NMR titration. In the titration, perturbations were observed not only for peak positions but also for peak intensities in the HSQC spectrum of Bcl-xL (Figure 2A–C). The peak intensities were significantly decreased because of the increase in the apparent molecular size upon formation of the complex between Bcl-xL and the p53 DBD, which was not observed in the titration of Mcl-1 with the p53 DBD (Figure 2H). Because the same molecular ratio was used in the titrations of Mcl-1 and Bcl-xL with the p53 DBD, this confirms that the binding affinity of the p53 DBD for Bcl-xL is much higher than for Mcl-1. Mapping the chemical shift perturbations onto the structure of Bcl-xL reveals a negatively charged site composed of residues in helices α 1, α 5, and α 6 and in the loop between helices α 5 and α 6, which form a binding region for the p53 DBD on Bcl-xL. In addition, a number of residues buried in Bcl-xL also showed chemical shift changes, which suggests that conformational changes occur in Bcl-xL upon binding to the p53 DBD (Figure 2D). These results are consistent with previous NMR studies on the interaction between Bcl-xL and the p53 DBD.²⁴ The analysis indicates that a number of residues in Bcl-xL such as Val155, Asp156, and Glu158 involved in binding to the p53 DBD are not conserved in Mcl-1, in which the corresponding residues are Lys279, Thr280, and Asn282. The change from neutral or negatively charged residues in Bcl-xL to positively charged or neutral ones in Mcl-1 results in a significant reduction in the negative charge of the corresponding binding surface (Figure 2E,J), explaining the lower affinity of Mcl-1 for the p53 DBD.

The different binding affinities of Mcl-1 and Bcl-xL for the p53 DBD were further confirmed by ITC experiments (Figure 3). The dissociation constant for Bcl-xL and the p53 DBD

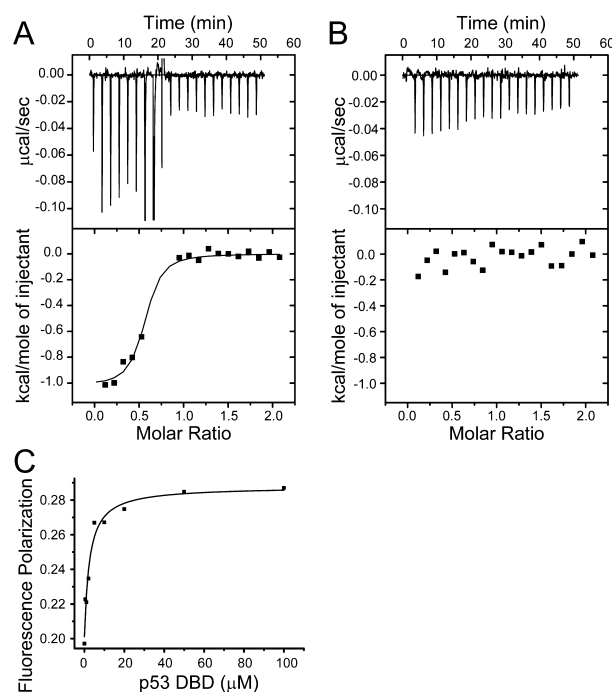


Figure 3. Isothermal titration calorimetry and fluorescence polarization results for the interaction of the p53 DBD with Bcl-xL and Mcl-1. The ITC experimental conditions (A, B) were 50 mM potassium phosphate (pH 7.2), 150 mM KCl, 5 mM β -mercaptoethanol at 20 °C. (A) Bcl-xL. (B) Mcl-1. (C) Fluorescence polarization measurement of the interaction between Bcl-xL and the p53 DBD.

determined from the ITC measurements is 594 ± 236 nM, which is similar to the value previously determined by surface plasmon resonance.^{38,39} The quality of the ITC titration curve was affected by protein precipitation, and therefore FP measurements were performed as an alternative approach to estimate the binding affinity between the p53 DBD and Bcl-xL. A dissociation constant of 2.5 ± 0.7 μM was obtained, which is similar to the previously reported values measured by FP.²⁴ This confirms that the interaction between the p53 DBD and Bcl-xL is relatively strong. The dissociation constant for binding of Mcl-1 to the p53 DBD could not be derived from ITC experiments because the interaction was too weak and the heat change upon titration was too small (Figure 3). Considering the fact that the concentration of Mcl-1 used in the NMR titration was 100 μM , the K_d value is likely to be in the mM range, which suggests that the binding affinities of the p53 DBD for Mcl-1 and Bcl-xL differ by at least 1000-fold (Table 1). The

Table 1. Dissociation Constants for Interaction of Bcl-xL and Mcl-1 with p53

p53 domain	Bcl-xL	Mcl-1
DBD (94–312)	594 ± 236 nM (ITC) 2.5 ± 0.7 μM (FP)	$\gg 100$ μM (ITC/NMR)
TAD (1–73)	294 ± 37 μM (ITC) 462 ± 45 μM (NMR)	24 ± 4 μM (ITC) 6.7 ± 6.6 μM (NMR)
TAD1 (1–40)	260 μM (NMR) ^a	616 ± 132 μM (NMR)
TAD2 (37–61)	7.5 ± 2.7 mM (NMR)	26.6 ± 6.9 μM (NMR)

^aValue for p53 (15–29) and Bcl-xL interaction from ref 26.

weak affinity of Mcl-1 for the p53 DBD implies that the interaction of Mcl-1 with the p53 DBD may not occur under physiological conditions, in contrast to the important interaction of Bcl-xL with the p53 DBD.

Binding Affinity of the p53 Transcription Activation Domain Is Much Higher for Mcl-1 than for Bcl-xL. The p53 TAD can also interact with Bcl-xL as a BH3-like peptide to promote apoptosis.²⁶ Therefore, we analyzed the interactions of the p53 TAD with Mcl-1 and with Bcl-xL by ITC (Figure 4). The results indicate that both Bcl-xL and Mcl-1 can interact with the p53 TAD, but the affinities are significantly different. The equilibrium dissociation constant (K_d) obtained for binding of Bcl-xL to the p53 TAD was 294 ± 37 μM , which

is similar to the reported value (260 μM) for binding of Bcl-xL to p53 SN15 (15–29) obtained by NMR titration.²⁶ The K_d for the binding of Mcl-1 to the p53 TAD is 24 ± 4 μM , which represents a more than ten times higher affinity than for binding of Bcl-xL to the p53 TAD (Table 1).

The above data demonstrate that Bcl-xL binds much more strongly to the p53 DBD ($K_d \sim 200$ nM) than to the p53 TAD ($K_d \sim 300$ μM). In contrast, the binding of Mcl-1 to the p53 DBD ($K_d \gg 100$ μM) was much weaker than to the p53 TAD ($K_d \sim 10$ – 20 μM). Therefore, the p53 DBD is the preferred binding region for Bcl-xL, whereas the p53 TAD is the preferred binding region for Mcl-1.

p53 Transcription Activation Domain Binds to the BH3-Binding Groove of Mcl-1. The binding site of the p53 TAD on Mcl-1 was detected using two-dimensional ^1H – ^{15}N HSQC spectra of uniformly ^{15}N -labeled Mcl-1 recorded in the presence of different concentrations of unlabeled p53 TAD (Figure 5E,F). A number of peaks in the spectra of Mcl-1 showed chemical shift changes upon p53 TAD binding. From the chemical shift changes of five representative residues (V216, G219, Q221, I237, I264), an average value (6.7 ± 6.6 μM) of the dissociation constant was obtained (Figure 5G). This is consistent with the results of ITC measurements. Residues of Mcl-1 with chemical shift perturbations ($\Delta\delta$) greater than the average ($0.085 > \Delta\delta > 0.046$ ppm) and those greater than one standard deviation ($\Delta\delta > 0.085$ ppm) were mapped onto the human Mcl-1 structural model (Figure 5H). Figure 5H shows that these residues are mainly located in the BH3-binding groove formed by the BH1, BH2, and BH3 regions, along with the segment between BH3 and BH1 including helices $\alpha 3$ and $\alpha 4$ and the loop between them, as well as the C-terminus of helix $\alpha 6$.

It has been reported that the p53 TAD can bind to the BH3-binding groove of Bcl-xL,²⁶ but in another report, no interaction was observed.^{11,37} To investigate this further, we studied the interaction between Bcl-xL and the p53 TAD by NMR titration (Figure 5A,B). The results show that the p53 TAD can interact with Bcl-xL, with a K_d value of 462 ± 45 μM (Figure 5C), which is slightly weaker than the interaction of Bcl-xL with p53 SN15 (residues 15–29 of p53), for which a K_d value of 260 μM was obtained from NMR titration.²⁶ The chemical shift perturbation mapping indicates that the p53 TAD binding site on Bcl-xL is the BH3-binding groove (Figure 5D), which is in agreement with previous studies.^{26,27} Therefore, the BH3 grooves are the binding sites for the p53 TAD in the case of both Bcl-xL and Mcl-1. Further, the results of ITC and NMR studies demonstrate that Bcl-xL and Mcl-1 have different binding affinities for the p53 TAD (Table 1).

p53 TAD2 Has a Stronger Binding Affinity than TAD1 for Mcl-1. The p53 TAD contains two subdomains, TAD1 (residue 1–40) and TAD2 (residues 40–61). The previous NMR titration studies indicate that the spectra of both TAD1 and TAD2 are perturbed by addition of Bcl-xL; however, TAD1 is the preferred Bcl-xL binding site in the p53 TAD.^{26,27} To define the binding site for Mcl-1 on the p53 TAD, the two-dimensional ^1H – ^{15}N HSQC spectra of ^{15}N -labeled p53 TAD (residues 1–73) in the absence and presence of Mcl-1 were recorded. The spectra revealed significant chemical shift perturbations of resonances for residues in segments 18–26 and 45–56 of TAD1 and TAD2, respectively (Figure 6A,B,G), in particular for residues E51, Q52, W53, and F54 of TAD2. Therefore, both TAD1 and TAD2 subdomains interact with

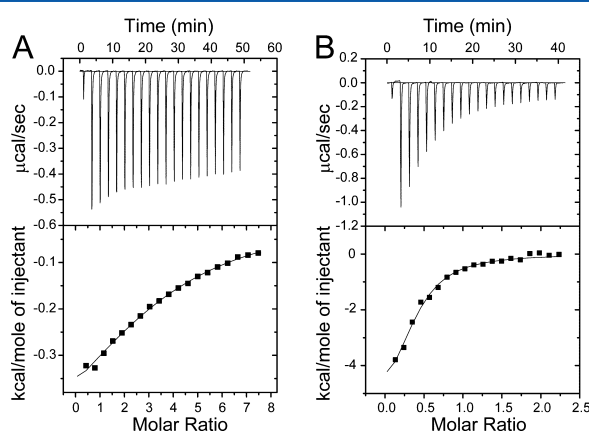


Figure 4. Isothermal titration calorimetry results for the interaction of Bcl-xL and Mcl-1 with the p53 TAD. The experimental conditions were 50 mM potassium phosphate (pH 6.5), 100 mM KCl at 25 °C. (A) Bcl-xL. (B) Mcl-1.

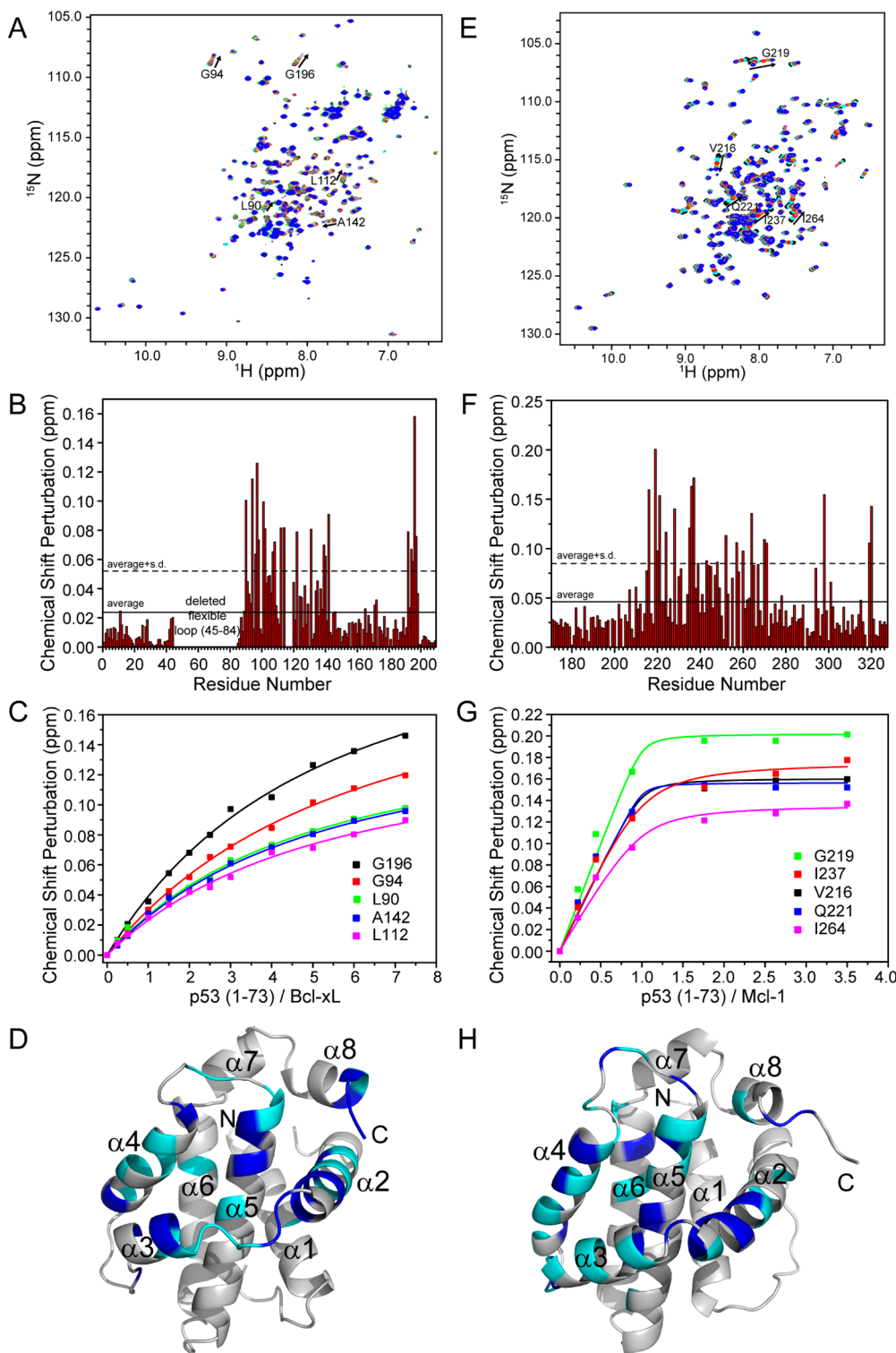


Figure 5. NMR titrations characterizing the interaction of Bcl-xL and Mcl-1 with the p53 TAD. (A–D) Bcl-xL. (E–H) Mcl-1. (A, E) ^1H - ^{15}N HSQC spectra of the titrations. (B, F) Chemical shift perturbations (CSP) versus residue number. (C, G) Dissociation constants obtained by fitting the titration curves. (D, H) Structural mappings of the chemical shift perturbations. Residues with a CSP value more than the average CSP value plus one standard deviation (average + s.d., dashed line in panels B and F) are shown in blue; those with a CSP value between the average CSP value (average, solid line in panels B and F) and the average CSP value plus one standard deviation are shown in cyan.

Mcl-1, but the more significant chemical shift perturbations for TAD2 suggests a higher binding affinity of Mcl-1 for TAD2.

In order to further confirm TAD2 as the preferred interaction site for Mcl-1, NMR titration of Mcl-1 with TAD1 or TAD2 was carried out. The K_d value obtained for

binding of p53 TAD2 to Mcl-1 was $26.6 \pm 6.9 \mu\text{M}$ (Figure 6F), which is only slightly weaker than that of the p53 TAD (residues 1–73) with Mcl-1 (Table 1). The K_d value for binding of p53 TAD1 to Mcl-1 was $616 \pm 132 \mu\text{M}$ (Figure 6E), which is more than 20 times weaker than that of binding of p53

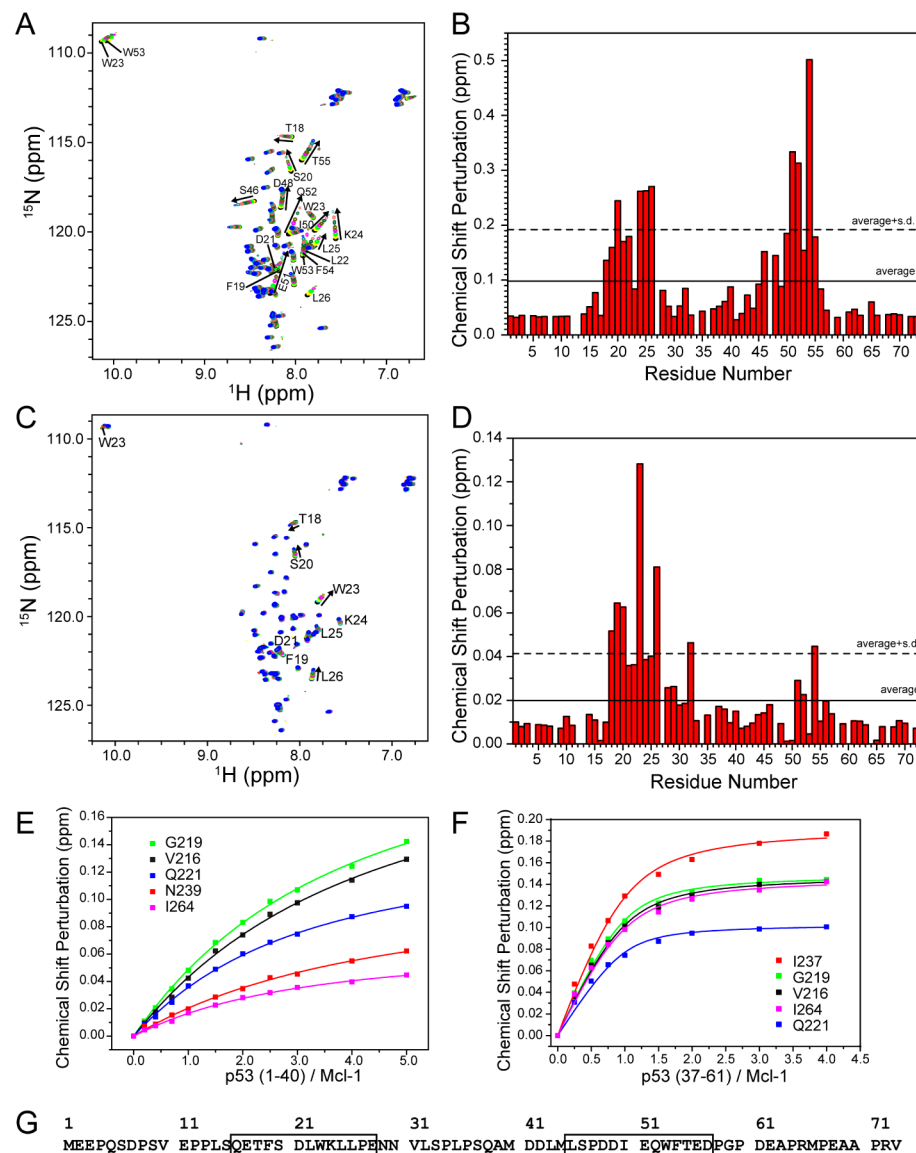


Figure 6. Mcl-1 binds with higher affinity to p53 TAD2 than to TAD1. (A) ^1H - ^{15}N HSQC spectra of the p53 TAD in the titrations with Mcl-1. (B) Chemical shift perturbations in the Mcl-1 titrations versus residue number of the p53 TAD. (C) ^1H - ^{15}N HSQC spectra of the p53 TAD in the titrations with Bcl-xL. (D) Chemical shift perturbations in the Bcl-xL titrations versus residue number of p53 TAD. (E, F) Dissociation constant for the interaction between p53 TAD1 (E) and TAD2 (F) with Mcl-1 as determined by fitting the titration curves for Mcl-1 with p53 TAD1 and TAD2, respectively. (G) Amino acid sequence of the p53 TAD (residues 1–73). The binding sites in the TAD1 and TAD2 subdomains are in boxes.

TAD2 to Mcl-1. This confirms that TAD2 is the preferred binding site for Mcl-1. The Bcl-xL binding site on the p53 TAD was also examined by NMR titration (Figure 6C,D). Similar to the previously reported results,^{26,27} TAD1 is the preferred binding site within the p53 TAD for Bcl-xL because resonances for residues in p53 TAD1 showed larger chemical shift perturbations on addition of Bcl-xL than residues in p53 TAD2. Further, NMR titrations indicated that the K_d value for the binding of p53 TAD2 to Bcl-xL is 7.5 ± 2.7 mM, which is much weaker than that for the binding of p53 TAD or p53 TAD1 to Bcl-xL (Table 1).

The binding sites on Mcl-1 for p53 TAD1 and TAD2 were revealed by the chemical shift perturbations, which are similar to those for binding of the intact p53 TAD with Mcl-1 (Figure 7A,C,E). Mapping the chemical shift perturbations onto the Mcl-1 structure indicates that the binding sites are located in the BH3 groove of Mcl-1 (Figure 7B,D,F). Therefore, binding

of p53 TAD1 and TAD2 occurs at the same site in Mcl-1, although TAD1 and TAD2 show different binding affinities for Mcl-1.

DISCUSSION

Previous studies demonstrated that p53 can interact with both Bcl-xL and Mcl-1, which have similar BH3-binding grooves. However, no reports have described the differences in binding features between these proteins. In this study, we have shown that Mcl-1 and Bcl-xL have different p53-binding profiles. The p53 DBD binds to Bcl-xL much more strongly than to Mcl-1, whereas the p53 TAD interacts with Mcl-1 with higher affinity than with Bcl-xL. In addition, although both proteins bind to the p53 TAD, Bcl-xL prefers to bind to TAD1 and Mcl-1 prefers to bind to TAD2. The different structural features of Bcl-xL and Mcl-1 can account for their different p53-binding features.

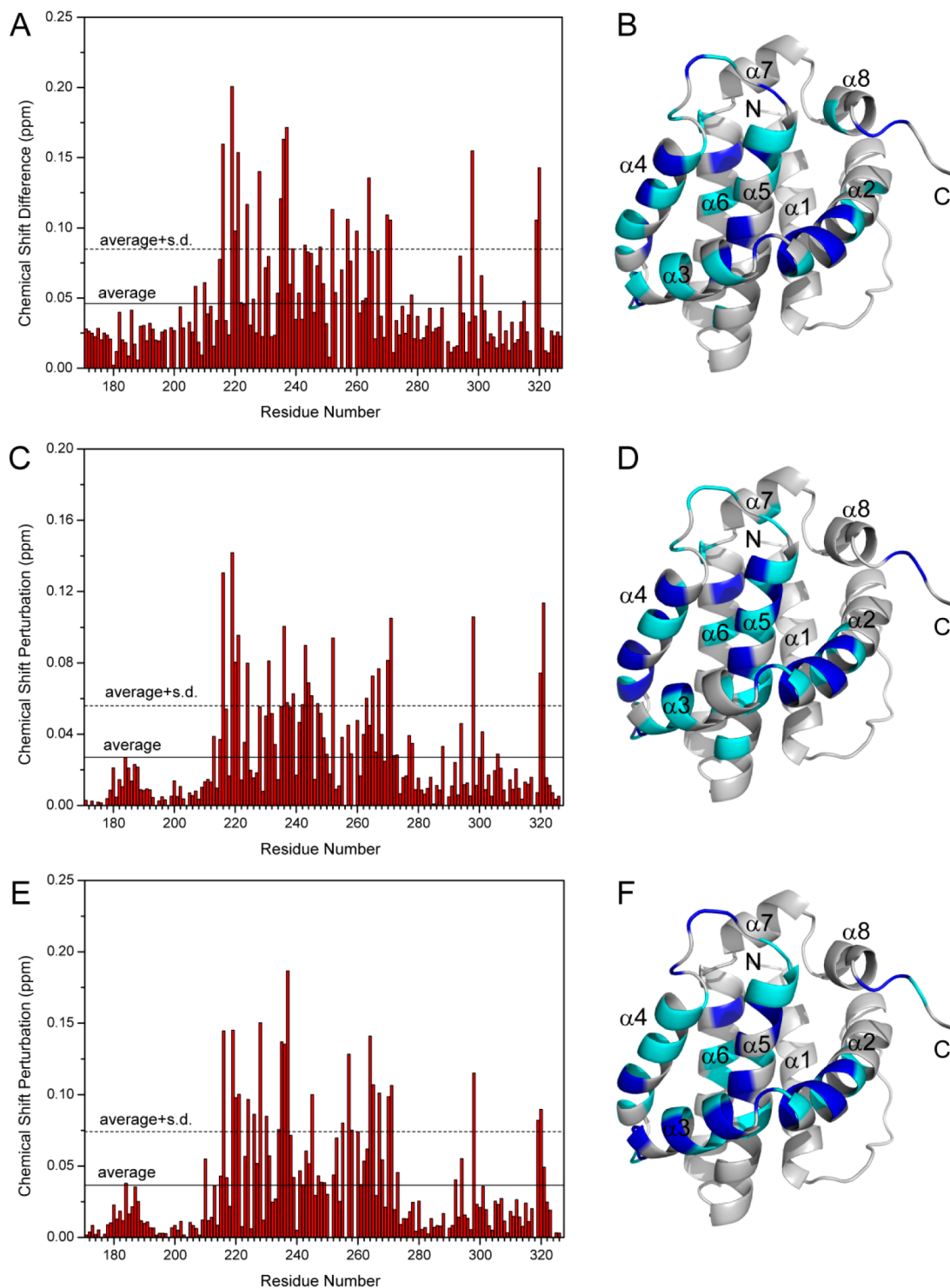


Figure 7. Comparison of the binding sites of p53 TAD (A, B), TAD1 (C, D), and TAD2 (E, F) on Mcl-1. The bar graphs of chemical shift perturbations (CSPs) versus residue number (left) are shown in panels A, C, and E, and the CSPs are mapped onto the structure of Mcl-1 (B, D, and F), in which residues with a CSP value more than the average CSP value plus one standard deviation (average + s.d., dashed line in panels A, C and E) are shown in blue and those with a CSP value between the average CSP value (average, solid line in panels A, C, and E) and the average CSP value plus one standard deviation are shown in cyan.

The interaction of Bcl-xL with p53, especially with the p53 DBD, has been extensively studied.^{11,24,37} The proposed physiological mechanism is that the binding of p53 changes the conformational state of the BH3-binding groove of Bcl-xL and increases the affinity of BH3 peptides for Bcl-xL, facilitating the interaction between Bcl-xL and BH3-only proteins. This in

turn displaces Bax/Bak from the anti-apoptotic Bcl-2 proteins and consequently promotes mitochondrial outer membrane permeabilization.²⁴ In our study, we found that the interaction between the p53 DBD and Mcl-1 is quite unlike the interaction between the p53 DBD and Bcl-xL. The interaction of the p53 DBD with Mcl-1 is quite weak and may have no physiological

role. Therefore, the physiological mechanism deduced from the interaction between Bcl-xL and the p53 DBD is probably not conserved in the interaction between Mcl-1 and the p53 DBD. The binding affinity of Mcl-1 for the p53 TAD ($K_d \sim 10\text{--}20 \mu\text{M}$) is much higher than that for binding to the p53 DBD ($K_d \gg 100 \mu\text{M}$) indicating the p53 TAD is the preferred binding site for Mcl-1. The affinity of Mcl-1 for the p53 TAD is similar to that measured for the binding of Bcl-xL to the p53 DBD at physiological salt concentration reported by Sot et al.³⁷ Therefore, the *in vivo* interaction of Mcl-1 and p53 is mainly mediated by the p53 TAD in a BH3-like manner, in which the p53 TAD binds to the BH3 groove of Mcl-1, similar to the mechanism observed for other BH3-containing proteins. This suggests that p53 is probably a competitor of pro-apoptosis BH3-containing proteins, allowing them to be released from Mcl-1. This competition mechanism in a cytosolic role of p53 was also proposed in a recent report that suggested that p53 can suppress the interaction of Mcl-1 with Bim, therefore releasing Bim to promote apoptosis.¹² However, the dissociation constant of Bim and Mcl-1 is in the range of $\sim 10 \text{ nM}$, which is much stronger than the interaction between p53 and Mcl-1, and further, the suppression occurs in mitochondria. Therefore, the physiological mechanism of cytosolic interaction between p53 and anti-apoptotic Bcl-2 family of proteins needs further study.

The p53 TAD interacts with many proteins. In most complexes, p53 TAD1 and/or TAD2 adopts a helical conformation. The interaction of p53 TAD1 with MDM2 is the most extensively investigated. The p53 TAD1 forms a short helix in the MDM2-p53 TAD1 complex,⁴⁰ and the binding is mainly through hydrophobic interactions. In most cases, the major driving force for binding of the p53 TAD with other proteins is the formation of hydrophobic and aromatic interactions.⁴¹ One exception is that the interaction between p53 TAD2 and programmed cell death 5 protein is dominated by electrostatic interactions.²⁹ On the other hand, the various BH3 peptides adopt a helical conformation when binding to Mcl-1 and other Bcl-2 family proteins, and more importantly, the two helices $\alpha 3$ and $\alpha 4$ in the Bcl-2 family proteins undergo conformational changes resulting in a wider groove for BH3 helix binding.^{13,42} BH3 peptides bind to the hydrophobic groove of Bcl-2 family proteins through a core hydrophobic interaction in the groove and polar interactions on the ridges. The combination of groove and ridge interactions defines the binding specificity.⁴² The interaction of p53 TAD2 with Mcl-1 is likely similar to the interaction between BH3 peptides and Bcl-2 family proteins involving several types of interactions. The sequences of p53 TAD1 and TAD2 are quite different, particularly in terms of polar residues (Figure 6G), which could explain the differences in affinity of p53 TAD1 and TAD2 for binding to Mcl-1. Thus, these polar interactions may also define the specificity of binding in the case of p53 TAD2 and Mcl-1. The atomic level details of the interactions between p53 TAD2 and Mcl-1 could be resolved by structure determination of the complex of p53 TAD2 and Mcl-1 by X-ray crystallography in the future.

BH3 mimetics represent a novel and exciting strategy in cancer therapeutic development. Targeting all of the anti-apoptotic Bcl-2 family proteins is important because of the overlapping compensatory functions of this protein family.⁴³ The different BH3-binding profiles of Mcl-1 and other Bcl-2 family members have been noted in structural and drug development studies.^{13,15,16,44} However, the observation of

different binding profiles of Mcl-1 and other Bcl-2 members to the same interacting protein has never been reported previously. The results in this paper not only confirm that Mcl-1 and Bcl-xL have different BH3-binding grooves, resulting in different p53-binding profiles, but also provide a new aspect to consider in drug design. Whether BH3 mimetics affect p53-mediated apoptosis should be carefully investigated in cancer therapeutic development. BH3 mimetics which block the BH3-binding groove could also suppress the interaction of p53 with Mcl-1 but not with Bcl-xL. The physiological effect of this difference needs further study, considering the complexity of p53-interaction networks.

The results in this paper indicate that Mcl-1 and Bcl-xL have different preferred binding sites on p53. This provides the possibility that p53 could bind Bcl-xL and Mcl-1 simultaneously. Because Bcl-xL and Mcl-1 have similar cytosolic and mitochondrial locations, the formation of the heterotrimer is possible *in vivo*. If p53 modulates the Bcl-2 family of proteins to promote apoptosis as proposed previously, then simultaneous binding would increase the efficiency of p53 utilization. Increased efficiency by simultaneous binding may be common in cytosolic p53 functions because of the existence of numerous p53-binding partners.

■ AUTHOR INFORMATION

Corresponding Authors

*J. Wang. E-mail: jfw@sun5.ibp.ac.cn. Phone: +86-10-6488 8498. Fax: +86-10-6487 2026.

*Y. Feng. E-mail: fengyg@qibebt.ac.cn. Phone: +86-532-8066 2706. Fax: +86-532-8066 2707.

Author Contributions

[†]Both authors contributed equally to this work.

Funding

This research was supported by grants from the National Natural Science Foundation of China to Y.F. (30800179 and 30970571) and J.W. (30170201 and 30770434), the 973 Program of China to B.X. (2012CB910700), the Beijing Natural Science Foundation to Y.F. (5092018), and the China Postdoctoral Science Foundation to H.Y. (20090460350).

Notes

The authors declare no competing financial interest.

■ ACKNOWLEDGMENTS

We thank Qian Liu and Prof. Kalle Gehring, McGill University, Canada, for providing the chemical shift assignments of cMcl-1. We thank Dr. Si Wu, Institute of Biophysics, Chinese Academy of Sciences, for help with the fluorescence polarization measurements.

■ ABBREVIATIONS

BH, Bcl-2 homology; DBD, DNA-binding domain; TAD, transactivation domain; ITC, isothermal titration calorimetry; HSQC, heteronuclear single quantum correlation; CSP, chemical shift perturbations; FP, fluorescence polarization; BFP, blue fluorescent protein

■ REFERENCES

- Riley, T., Sontag, E., Chen, P., and Levine, A. (2008) Transcriptional control of human p53-regulated genes. *Nat. Rev. Mol. Cell Biol.* 9, 402–412.
- Youssen, K. H., and Prives, C. (2009) Blinded by the light: The growing complexity of p53. *Cell* 137, 413–431.

- (3) Speidel, D. (2010) Transcription-independent p53 apoptosis: an alternative route to death. *Trends Cell Biol.* 20, 14–24.
- (4) Chipuk, J. E., and Green, D. R. (2003) p53's believe it or not: Lessons on transcription-independent death. *J. Clin. Immunol.* 23, 355–361.
- (5) Vaseva, A. V., and Moll, U. M. (2009) The mitochondrial p53 pathway. *Biochim. Biophys. Acta, Bioenerg.* 1787, 414–420.
- (6) Green, D. R., and Kroemer, G. (2009) Cytoplasmic functions of the tumour suppressor p53. *Nature* 458, 1127–1130.
- (7) Youle, R. J., and Strasser, A. (2008) The BCL-2 protein family: opposing activities that mediate cell death. *Nat. Rev. Mol. Cell Biol.* 9, 47–59.
- (8) Danial, N. N. (2007) BCL-2 family proteins: Critical checkpoints of apoptotic cell death. *Clin. Cancer. Res.* 13, 7254–7263.
- (9) Leu, J. I. J., Dumont, P., Hafey, M., Murphy, M. E., and George, D. L. (2004) Mitochondrial p53 activates Bak and causes disruption of a Bak-Mcl1 complex. *Nat. Cell Biol.* 6, 443–450.
- (10) Chipuk, J. E., Kuwana, T., Bouchier-Hayes, L., Droin, N. M., Newmeyer, D., Schuler, M., and Green, D. R. (2004) Direct activation of Bax by p53 mediates mitochondrial membrane permeabilization and apoptosis. *Science* 303, 1010–1014.
- (11) Mihara, M., Erster, S., Zaika, A., Petrenko, O., Chittenden, T., Pancoska, P., and Moll, U. M. (2003) p53 has a direct apoptogenic role at the mitochondria. *Mol. Cell* 11, 577–590.
- (12) Han, J., Goldstein, L. A., Hou, W., Gastman, B. R., and Rabinowich, H. (2010) Regulation of mitochondrial apoptotic events by p53-mediated disruption of complexes between anti-apoptotic Bcl-2 members and Bim. *J. Biol. Chem.* 285, 22473–22483.
- (13) Fire, E., Gulla, S. V., Grant, R. A., and Keating, A. E. (2010) Mcl-1-Bim complexes accommodate surprising point mutations via minor structural changes. *Protein Sci.* 19, 507–519.
- (14) Thomas, L. W., Lam, C., and Edwards, S. W. (2010) Mcl-1; the molecular regulation of protein function. *FEBS Lett.* 584, 2981–2989.
- (15) Chen, L., Willis, S. N., Wei, A., Smith, B. J., Fletcher, J. I., Hinds, M. G., Colman, P. M., Day, C. L., Adams, J. M., and Huang, D. C. S. (2005) Differential targeting of prosurvival Bcl-2 proteins by their BH3-only ligands allows complementary apoptotic function. *Mol. Cell* 17, 393–403.
- (16) Dutta, S., Gulla, S., Chen, T. S., Fire, E., Grant, R. A., and Keating, A. E. (2010) Determinants of BH3 binding specificity for Mcl-1 versus Bcl-x(L). *J. Mol. Biol.* 398, 747–762.
- (17) Oltersdorf, T., Elmore, S. W., Shoemaker, A. R., Armstrong, R. C., Augeri, D. J., Belli, B. A., Bruncko, M., Deckwerth, T. L., Dinges, J., Hajduk, P. J., Joseph, M. K., Kitada, S., Korsmeyer, S. J., Kunzer, A. R., Letai, A., Li, C., Mitten, M. J., Nettesheim, D. G., Ng, S., Nimmer, P. M., O'Connor, J. M., Oleksijew, A., Petros, A. M., Reed, J. C., Shen, W., Tahir, S. K., Thompson, C. B., Tomaselli, K. J., Wang, B. L., Wendt, M. D., Zhang, H. C., Fesik, S. W., and Rosenberg, S. H. (2005) An inhibitor of Bcl-2 family proteins induces regression of solid tumours. *Nature* 435, 677–681.
- (18) van Delft, M. F., Wei, A. H., Mason, K. D., Vandenberg, C. J., Chen, L., Czabotar, P. E., Willis, S. N., Scott, C. L., Day, C. L., Cory, S., Adams, J. M., Roberts, A. W., and Huang, D. C. S. (2006) The BH3 mimetic ABT-737 targets selective Bcl-2 proteins and efficiently induces apoptosis via Bak/Bax if Mcl-1 is neutralized. *Cancer Cell* 10, 389–399.
- (19) Deng, J., Carlson, N., Takeyama, K., Dal Cin, P., Shipp, M., and Letai, A. (2007) BH3 profiling identifies three distinct classes of apoptotic blocks to predict response to ABT-737 and conventional chemotherapeutic agents. *Cancer Cell* 12, 171–185.
- (20) Vikstrom, I., Carotta, S., Luthje, K., Peperzak, V., Jost, P. J., Glaser, S., Busslinger, M., Bouillet, P., Strasser, A., Nutt, S. L., and Tarlinton, D. M. (2010) Mcl-1 is essential for germinal center formation and B cell memory. *Science* 330, 1095–1099.
- (21) Germain, M., Nguyen, A. P., Le Grand, J. N., Arbour, N., Vanderluit, J. L., Park, D. S., Opferman, J. T., and Slack, R. S. (2011) MCL-1 is a stress sensor that regulates autophagy in a developmentally regulated manner. *EMBO J.* 30, 395–407.
- (22) Weng, S. Y., Yang, C. Y., Li, C. C., Sun, T. P., Tung, S. Y., Yen, J. J. Y., Tsai, T. F., Chen, C. M., Chen, S. H., Hsiao, M., Huang, P. H., and Yang-Yen, H. F. (2011) Synergism between p53 and Mcl-1 in protecting from hepatic injury, fibrosis and cancer. *J. Hepatol.* 54, 685–694.
- (23) Xu, H. B., Tai, J., Ye, H., Kang, C. B., and Yoon, H. S. (2006) The N-terminal domain of tumor suppressor p53 is involved in the molecular interaction with the anti-apoptotic protein Bcl-XL. *Biochem. Biophys. Res. Commun.* 341, 938–944.
- (24) Hagn, F., Klein, C., Demmer, O., Marchenko, N., Vaseva, A., Moll, U. M., and Kessler, H. (2010) BclxL changes conformation upon binding to wild-type but not mutant p53 DNA binding domain. *J. Biol. Chem.* 285, 3439–3450.
- (25) Petros, A. M., Gunasekera, A., Xu, N., Olejniczak, E. T., and Fesik, S. W. (2004) Defining the p53 DNA-binding domain/Bcl-XL-binding interface using NMR. *FEBS Lett.* 559, 171–174.
- (26) Xu, H. B., Ye, H., Osman, N. E., Sadler, K., Won, E. Y., Chi, S. W., and Yoon, H. S. (2009) The MDM2-binding region in the transactivation domain of p53 also acts as a Bcl-X(L)-binding motif. *Biochemistry* 48, 12159–12168.
- (27) Ha, J. H., Won, E. Y., Shin, J. S., Jang, M., Ryu, K. S., Bae, K. H., Park, S. G., Park, B. C., Yoon, H. S., and Chi, S. W. (2011) Molecular mimicry-based repositioning of Nutlin-3 to anti-apoptotic Bcl-2 family proteins. *J. Am. Chem. Soc.* 133, 1244–1247.
- (28) Cheng, Y., and Patel, D. J. (2004) An efficient system for small protein expression and refolding. *Biochem. Biophys. Res. Commun.* 317, 401–405.
- (29) Yao, H. W., Feng, Y. G., Zhou, T., Wang, J. F., and Wang, Z. X. (2012) NMR studies of the interaction between human programmed cell death 5 and human p53. *Biochemistry* 51, 2684–2693.
- (30) Johnson, B. A., and Blevins, R. A. (1994) NMRView - a computer program for the visualization and analysis of NMR data. *J. Biomol. NMR* 4, 603–614.
- (31) Lei, X. B., Chen, Y. Y., Du, G. H., Yu, W. Y., Wang, X. H., Qu, H., Xia, B., He, H. P., Mao, J. H., Zong, W. X., Liao, X. D., Mehrpour, M., Hao, X. J., and Chen, Q. (2006) Gossypol induces Bax/Bak-independent activation of apoptosis and cytochrome c release via a conformational change in Bcl-2. *FASEB J.* 20, 2147–2149.
- (32) Liu, Q., Moldoveanu, T., Sprules, T., Matta-Camacho, E., Mansur-Azzam, N., and Gehring, K. (2010) Apoptotic regulation by MCL-1 through heterodimerization. *J. Biol. Chem.* 285, 19615–19624.
- (33) Grzesiek, S., Stahl, S. J., Wingfield, P. T., and Bax, A. (1996) The CD4 determinant for downregulation by HIV-1 Nef directly binds to Nef. Mapping of the Nef binding surface by NMR. *Biochemistry* 35, 10256–10261.
- (34) Fielding, L. (2007) NMR methods for the determination of protein-ligand dissociation constants. *Prog. Nucl. Magn. Reson. Spectrosc.* 51, 219–242.
- (35) Day, C. L., Chen, L., Richardson, S. J., Harrison, P. J., Huang, D. C. S., and Hinds, M. G. (2005) Solution structure of prosurvival Mcl-1 and characterization of its binding by proapoptotic BH3-only ligands. *J. Biol. Chem.* 280, 4738–4744.
- (36) Sali, A., and Blundell, T. L. (1993) Comparative protein modeling by satisfaction of spatial restraints. *J. Mol. Biol.* 234, 779–815.
- (37) Sot, B., Freund, S. M. V., and Fersht, A. R. (2007) Comparative biophysical characterization of p53 with the proapoptotic BAK and the antiapoptotic BCL-x(L). *J. Biol. Chem.* 282, 29193–29200.
- (38) Chipuk, J. E., Bouchier-Hayes, L., Kuwana, T., Newmeyer, D. D., and Green, D. R. (2005) PUMA couples the nuclear and cytoplasmic pro-apoptotic function of p53. *Science* 309, 1732–1735.
- (39) Tomita, Y., Marchenko, N., Erster, S., Nemajerova, A., Dehner, A., Klein, C., Pan, H. G., Kessler, H., Pancoska, P., and Moll, U. M. (2006) WT p53, but not tumor-derived mutants, bind to Bcl2 via the DNA binding domain and induce mitochondrial permeabilization. *J. Biol. Chem.* 281, 8600–8606.
- (40) Kussie, P. H., Gorina, S., Marechal, V., Elenbaas, B., Moreau, J., Levine, A. J., and Pavletich, N. P. (1996) Structure of the MDM2

oncoprotein bound to the p53 tumor suppressor transactivation domain. *Science* 274, 948–953.

(41) Joerger, A. C., and Fersht, A. R. (2010) The tumor suppressor p53: from structures to drug discovery. *Cold Spring Harbor Perspect. Biol.* 2, a000919.

(42) Chipuk, J. E., Moldoveanu, T., Llambi, F., Parsons, M. J., and Green, D. R. (2010) The BCL-2 Family Reunion. *Mol. Cell* 37, 299–310.

(43) Quinn, B. A., Dash, R., Azab, B., Sarkar, S., Das, S. K., Kumar, S., Oyesanya, R. A., Dasgupta, S., Dent, P., Grant, S., Rahmani, M., Curiel, D. T., Dmitriev, I., Hedvat, M., Wei, J., Wu, B., Stebbins, J. L., Reed, J. C., Pellecchia, M., Sarkar, D., and Fisher, P. B. (2011) Targeting Mcl-1 for the therapy of cancer. *Expert Opin. Invest. Drugs* 20, 1397–1411.

(44) Zhang, Z., Yang, H., Wu, G., Li, Z., Song, T., and Li, X. Q. (2011) Probing the difference between BH3 groove of Mcl-1 and Bcl-2 protein: Implications for dual inhibitors design. *Eur. J. Med. Chem.* 46, 3909–3916.